2012-4

Analysis of a Kinetic Multi-Segment Foot Model. Part II: Kinetics and Clinical Implications

Dustin A. Bruening
dabruening@byu.edu

Kevin M. Cooney

Frank L. Buczek

Original Publication Citation

Bruening DA, Cooney KM, Buczek FL. Analysis of a kinetic multi-segment foot model part II: kinetics and clinical implications. Gait Posture. 2012 Apr;35(4):535-40. doi: 10.1016/j.gaitpost.2011.11.012. Epub 2011 Dec 23.

Analysis of a kinetic multi-segment foot model part II: Kinetics and clinical implications

Dustin A. Bruening, Kevin M. Cooney, Frank L. Buczek

Abstract

Kinematic multi-segment foot models have seen increased use in clinical and research settings, but the addition of kinetics has been limited and hampered by measurement limitations and modeling assumptions. In this second of two companion papers, we complete the presentation and analysis of a three segment kinetic foot model by incorporating kinetic parameters and calculating joint moments and powers. The model was tested on 17 pediatric subjects (ages 7–18 years) during normal gait. Ground reaction forces were measured using two adjacent force platforms, requiring targeted walking and the creation of two sub-models to analyze ankle, midtarsal, and 1st metatarsophalangeal joints. Targeted walking resulted in only minimal kinematic and kinetic differences compared with walking at self-selected speeds. Joint moments and powers were calculated and ensemble averages are presented as a normative database for comparison purposes. Ankle joint powers are shown to be overestimated when using a traditional single-segment foot model, as substantial angular velocities are attributed to the mid-tarsal joint. Power transfer is apparent between the 1st metatarsophalangeal and mid-tarsal joints in terminal stance/pre-swing. While the measurement approach presented here is limited to clinical populations with only minimal impairments, some elements of the model can also be incorporated into routine clinical gait analysis.

Keywords: Multi-segment foot; Foot models; Gait analysis; Kinetics

Introduction

Kinematic multi-segment foot models have been increasingly used in clinical gait analysis and human movement research; however, the addition of kinetics to multi-segment foot modeling has been limited and hampered by force measurement limitations [1], [2] and [3] and unproven modeling assumptions [4]. Scott and Winter [5] created an early kinetic model, calculating moments for eight separate foot joints. Analysis was confined to two-dimensions and force measurement methodology required the superposition of multiple trials interacting with a small custom-built force sensor. MacWilliams et al. [6] later proposed the only three-dimensional kinetic model found in the literature. Sixteen markers were used to create eight segments, requiring many assumptions on joint motion. To measure subarea forces, pressure and force data from separate trials were combined using an estimation method [1] and [3], and the mediolateral

forces between segments were neglected when calculating joint moments [2]. Given the limitations in repeatability and force measurement technology, these models may be too complex for use in clinical analysis.

The addition of kinetics to multi-segment foot modeling may provide additional insight into foot and ankle function as well as influence the evolution of multi-segment foot models. Measurement limitations may be more readily overcome and model parameters more robustly implemented in a model that is simpler than those previously attempted. In part I of this two-part study, a three-segment foot model was described and analyzed. Segment reference frames and joint centers were defined for use with inverse dynamics methods, and the model's kinematic behavior was characterized during normal gait. Segment rigidity analysis showed deformable behavior for the Forefoot segment during transitions between stance and swing, which should be kept in mind when evaluating angular velocities and joint powers (i.e. dependent on chosen tracking markers). In this companion paper, additional parameters needed for inverse dynamics calculations are defined, ground reaction forces are measured, and model kinetics are calculated. Implications for clinical gait analysis are discussed.

Methods

Overview

A particular hurdle in calculating multi-segment foot kinetics is measuring the complete ground reaction forces (GRFs comprising normal forces, shear forces, and a free moment) under each segment, as there are currently no commercially available devices capable of subarea GRF measurement. In this study, we chose to use two adjacent force platforms to directly measure GRFs. Practically, this required visual targeting of the force platforms; and because only two segments could be evaluated at a time, it required the creation of two sub-models. Due to these restrictions, we felt it important to secondarily assess the effects of visual targeting as well as the contributions that foot inertial parameters add to multi-segment foot kinetic calculations. The methods section will begin by defining the sub-models and associated parameters not previously addressed in part I, then describe the GRF measurement methodology, and end with the calculation of kinetic parameters and evaluation of the above mentioned secondary analyses.

Model

The full three segment foot model includes Shank, Hindfoot, Forefoot, and Hallux segments (as well as a traditional rigid Foot segment), separated by the ankle, mid-tarsal, and 1st metatarsophalangeal (MP) joints respectively. Marker conventions, joint centers, and segment reference frames were defined in part I. Three kinetic sub-models were then created: (1) the MID model included the Shank, Hindfoot, and Forefoot, allowing for mid-tarsal joint analysis; (2) the TOE model included the Shank, Foot, and Hallux, and allowed for MP joint analysis; (3) the FOOT model, comprised of the Shank and Foot segments, was used to analyze the effects of segmentation on kinetic results. For each of these three kinetic models (Fig. 1), kinematic-only definitions of all segment reference frames (Shank, Hindfoot, Forefoot, Hallux, Foot) were also included. Segment inertial parameters were implemented in the following manner: the masses of the Shank and Foot were taken from Dempster [7], and the Foot mass was then partitioned

among the foot segments of each model (Hindfoot, Forefoot, and/or Hallux) in the same ratios as their respective volumes, modeling each as simple geometric solids with uniform densities (Fig. 1). Inertia tensors for each segment were calculated from the geometric solids and associated masses [8].

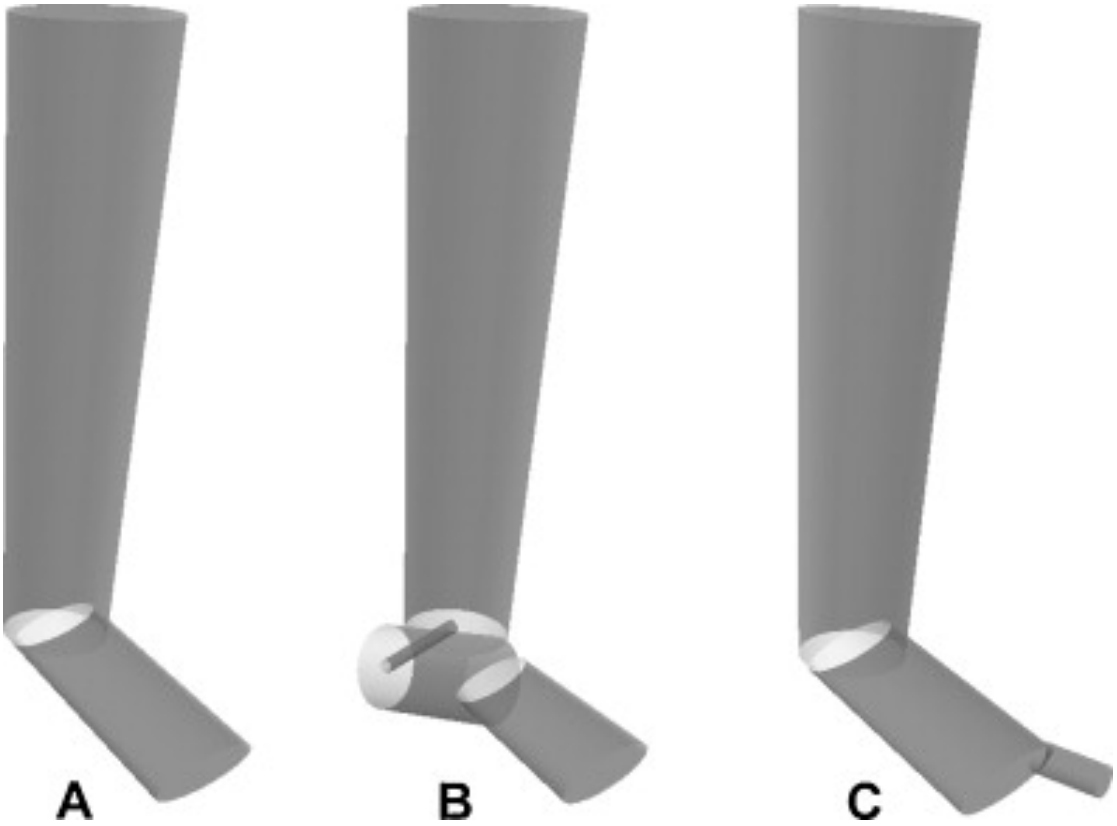

Fig. 1. *Three sub-models used in the study: (A) traditional single segment foot (FOOT model); (B) mid-tarsal model (MID model), including Hindfoot and Forefoot; and (C) metatarsophalangeal model (TOE model), including Foot and Hallux. Segment volumes were calculated from simple geometric shapes, with lengths equal to the segments' long axis. Rearfoot was modeled as a cylinder with diameter equal to the distance between markers LC and MC. Forefoot was modeled as an elliptical cylinder with major diameter equal to the distance between markers NV and CU, and minor diameter equal to the height of H2. Hallux was modeled as a cylinder with diameter equal to the height of HX. Also note that we used a near mass-less dummy segment in the MID model so the ankle joint moment could be calculated at the correct point using commercial software.*

Subjects and measurement protocol

Seventeen healthy pediatric participants (9M/8F; age 12.6 ± 3.4 yrs; height 154 ± 18 cm; weight 48 ± 17 kg; mean ± SD) volunteered and signed consent/assent forms approved by the local human subjects ethics committee. The participants and equipment setup were identical to those from the kinematic validity protocol in part I.

Participants first walked at a self-selected speed across a floor containing two adjacent (gap of ≈2 mm) AMTI OR6-7-100 force platforms (AMTI, Watertown MA, USA). The platforms were covered with a 2 mm thick tile overlay, accounted for by the motion capture system. Three trials were collected during which the entire foot made contact with a single force platform. Next, participants walked using a three-step targeting approach so that specified portions of the foot contacted the adjacent platforms. To evaluate the mid-tarsal joint (MID model trials), the Hindfoot contacted the first platform while the rest of the foot contacted the second platform, with the platform division at approximately the mid-tarsal joint. To evaluate the MP joint (TOE model trials), the division was just distal to the metatarsal heads, with the hallux and toes isolated on the second platform. For both trial types, a foot outline was drawn on the platforms for visual guidance, but participants were instructed to walk as normally as possible and the starting position was adjusted until the appropriate placement was achieved. Numerous trials (typically between 15 and 30) were collected until at least three (for each trial type) were identified with accurate foot placement, which was verified by two video cameras located on either side of the platform division (Fig. 2).

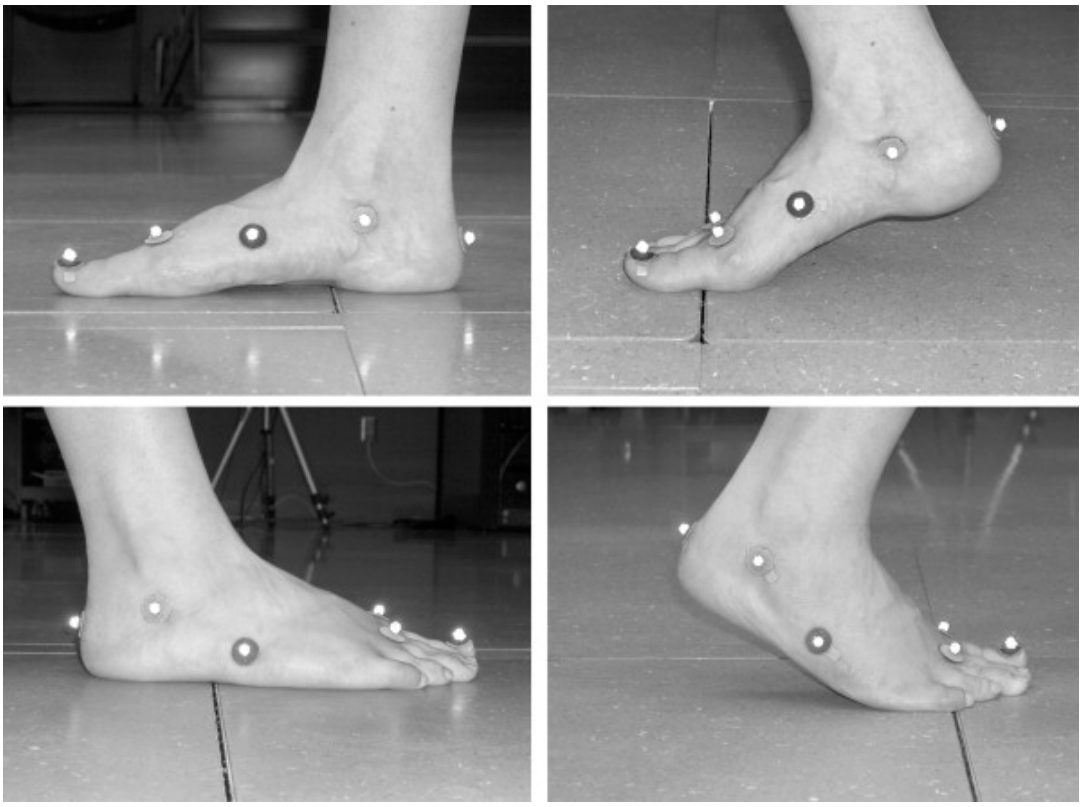

Fig. 2. *Example photographs showing targeted foot placement spanning two adjacent force platforms. Left panels: MID model trial, right panels: TOE model trial.*

Data analysis

Visual3D software (C-motion, Inc., Germantown, MD, USA) was used to create all models and perform all calculations. Marker trajectories were collected at 120 Hz and filtered using a low pass Butterworth filter (6 Hz cutoff frequency). GRF data were collected at 1560 Hz. For the targeted trials, the channels from the two force platforms were also combined to create a single virtual platform that could be used with the FOOT model. Both individual and virtual platform GRF data were then filtered using a low pass Butterworth filter (100 Hz cutoff frequency), and a threshold cutoff of 5 N was applied to avoid center of pressure errors at low force values.

Joint angles were calculated between distal and proximal (reference) segments using Cardan angles as in part I. Net joint moments were calculated at the proximal end of each kinetic segment using traditional inverse dynamics, and expressed for each joint in the same segment reference frames as the kinematics (i.e. segment proximal to the joint). Total joint power was calculated as the dot product of the joint moment and joint angular velocity vectors, while the three individual terms of the dot product were associated with the specific orthogonal axes. All variables were time-normalized to percent stance for between-trial comparisons, and all kinetic measures were normalized by subject mass for between-subject comparisons.

For each subject, three representative trials were chosen (one for each trial type). This was done manually for the self-selected speed trials, visually evaluating kinematic and kinetic variables. For the MID model trials and TOE model trials, this was done to minimize kinetic differences, in the following manner: ensemble averages were calculated for each GRF component across the three self-selected speed trials. Root mean square (RMS) differences were then calculated between virtual GRF components from the MID and TOE trials and the ensemble averaged GRFs from the self-selected speed trials. The trial with the smallest RMS differences across all GRF components was chosen as representative for that subject and trial type. Only the representative trials were used in all subsequent comparisons and to create group ensemble averages.

To help determine whether our targeted walking results were comparable to walking at a self-selected speed, representative MID model and TOE model trials were compared with representative self-selected speed walking trials using several key kinematic and kinetic variables. Discrete spatiotemporal parameters (stride length, stride time, and stance time) were compared statistically using two-tailed paired *t*-tests to determine trends, while joint angles and GRFs (virtual platform for targeted trials) were compared solely on a group basis using RMS differences (RMS difference of group ensemble averages).

To help quantify the contributions of foot inertial parameters on joint moment calculations, the FOOT model was additionally applied to the targeted trials. Using the virtual platform GRFs, ankle joint moments were calculated and compared between models (MID and FOOT, TOE and FOOT) applied to the same representative trials using root mean square (RMS) differences.

Results

Differences between targeted and self-selected speed walking variables were minimal (Table 1), although there were several statistically significant trends. Stride time tended to be slightly increased in the MID model trials, while stance time was slightly increased in both the MID model and TOE model trials (Table 1A). There were no statistical differences in stride length. Joint angle RMS differences (Table 1B) were less than or equal to 1.0° at the ankle and mid-tarsal joints (MID model trials), while the MP angle difference reached 2.2° in the sagittal plane (TOE model trials). This appeared to be due primarily to a slight decrease in peak dorsiflexion in the TOE model trials. Other than this specific difference, joint angles were nearly identical to those presented in part I, and are not displayed for brevity. Ground reaction force RMS differences (Table 1C) were less than 1% body weight (%BW) for all shear forces with the exception of the mediolateral forces from the TOE model trials (1.7%). Here, the anterior shear forces were slightly increased, although the patterns remained the same. Vertical force RMS differences were less than 5%BW for both trial types. Differences appeared to primarily occur at the force peaks.

Table 1. *Comparison of select kinematic and kinetic parameters between representative self-selected walking speed and targeted (MID model and TOE model) trials: (A) spatiotemporal metrics including mean, standard deviation, and p-value (calculated using paired t-tests between self-selected speed and targeted trials); (B) RMS differences between ensemble averaged joint angles (targeted ankle and mid-tarsal angles were calculated from MID model, while MP angles were calculated from TOE model); (C) RMS differences between ensemble averaged self-selected speed trial GRFs and targeted trial (virtual platform) GRFs.*

(A) Spatiotemporal metrics	**Self-selected**	**MID**	**TOE**
Stride length (m)	1.24 ± 0.10	1.27 ± 0.12 (p = 0.34)	1.26 ± 0.12 (p = 0.61)
Stride time (s)	0.95 ± 0.09	0.99 ± 0.06 (p = 0.02)	0.92 ± 0.22 (p = 0.46)
Stance time (s)	0.57 ± 0.07	0.60 ± 0.05 (p = 0.02)	0.61 ± 0.06 (p = 0.01)

(B) Joint angle RMS differences	**Sagittal plane**	**Coronal plane**	**Transverse plane**
Ankle	0.7°	0.8°	1.0°
Mid-tarsal	0.5°	0.3°	0.6°
MP	2.2°	0.6°	1.3°

(C) GRF RMS differences	**Medial/lateral**	**Anterior/posterior**	**Vertical**
MID model trials	0.8%BW	0.9%BW	3.6%BW
TOE model trials	1.7%BW	0.8%BW	4.2%BW

RMS differences in ankle moment magnitudes between the MID and FOOT models were 0.010 ± 0.003 Nm/kg, and between the TOE and FOOT models were 0.001 ± 0.000 Nm/kg. The latter two ankle moments were visually indistinguishable, while the former showed some minor differences at the signal peak, in pre-swing (graphs not displayed for brevity). These differences were generally less than 2% of the MID model peak value.

Subarea GRFs have been previously presented [1], and will not be reprinted for brevity. Net joint moments and component joint powers are presented as ensemble average curves (Fig. 3 and Fig. 4). Note that displayed ankle and mid-tarsal joint kinetics were calculated from the MID model trials, while MP joint kinetics were calculated from the TOE model trials. Group mean total joint powers were also superimposed on the same graph to show power interactions among joints (Fig. 5). Ankle power from the FOOT model applied to the MID model trials is also included for comparison.

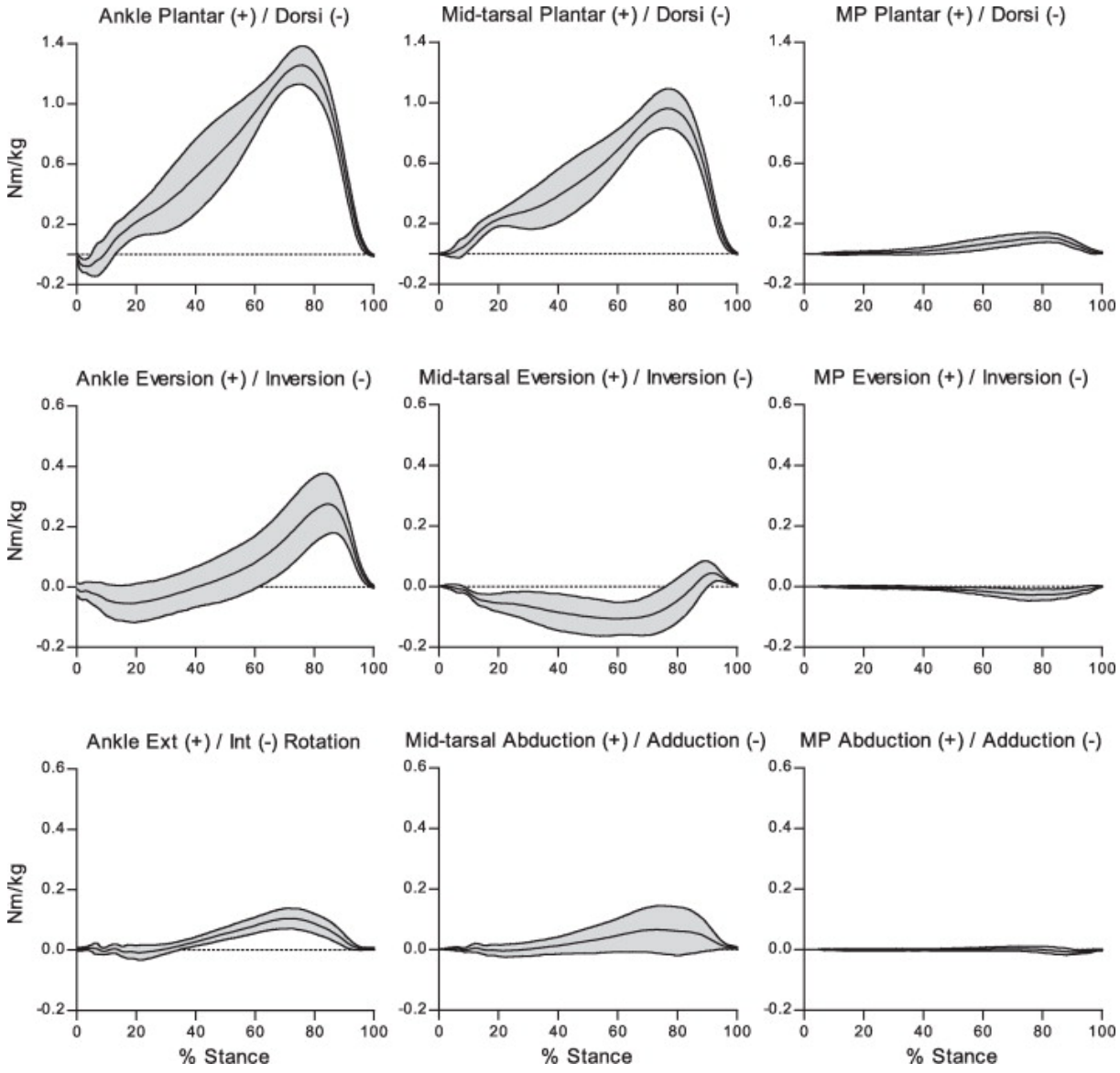

Fig. 3. *Ensemble average (mean ± standard deviation) net joint moments during normal gait (n = 17), time-normalized to percent stance. Joint moment conventions are intrinsic (i.e. calculated at the proximal end of the distal segment) and resolved in the proximal segment coordinate system. Ankle and mid-tarsal moments were calculated from MID model trials, while MP moments were calculated from TOE model trials.*

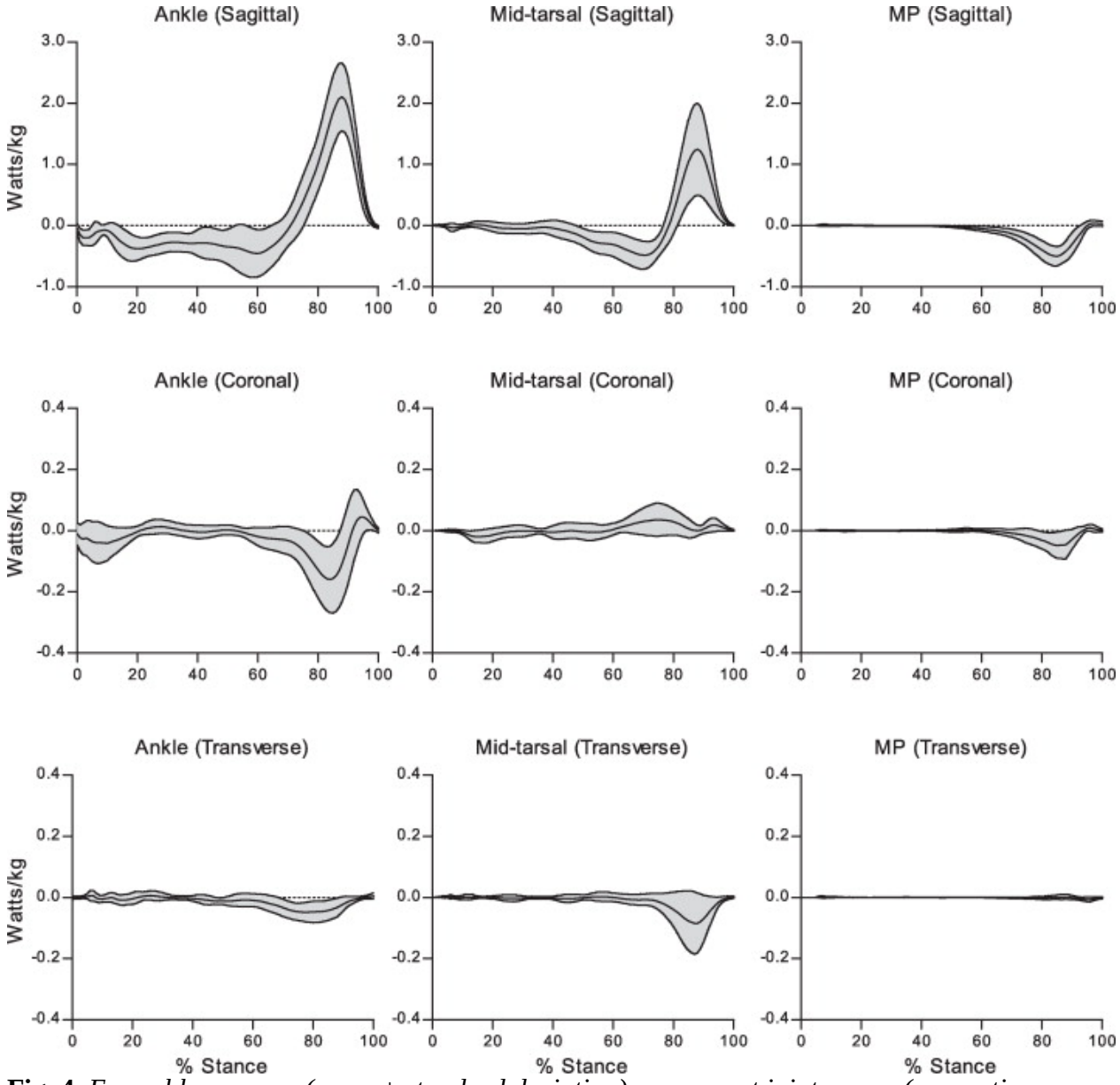

Fig. 4. *Ensemble average (mean ± standard deviation) component joint power (generation (+)/absorption (−)) during normal gait (n = 17), time-normalized to percent stance. Ankle and mid-tarsal powers were calculated from MID model trials, while MP powers were calculated from TOE model trials. For mid-tarsal powers, it should generally be noted that angular velocity will depend on the choice of Forefoot tracking markers due to the deformable nature of the Forefoot segment.*

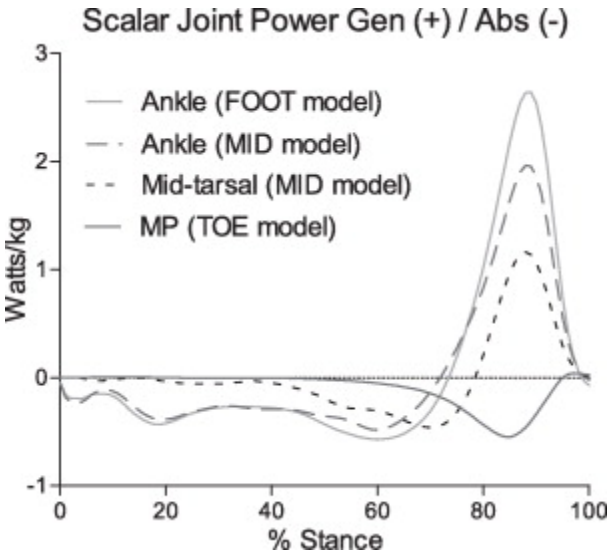

Fig. 5. *Mean (n = 17) total joint powers during normal gait. Ankle and mid-tarsal powers were calculated from MID model trials, while MP powers were calculated from TOE model trials. Ankle powers were also calculated using the FOOT model applied to the MID model trials for comparison.*

Discussion

This second of two companion papers completes the description and analysis of a three segment kinetic multi-segment foot model. While effort was made to accurately model multi-segment foot mass distributions and inertia tensors, these play a minimal role in inverse dynamics calculations compared with the dominant ground reaction force [9]. This was further confirmed in this study by the small differences found in the ankle joint moments between the MID and FOOT models and between the TOE and FOOT models, and allows for some flexibility in using various multi-segment foot sub-models as we have done. Foot inertial parameters may have a larger role in more dynamic activities such as running and jumping.

As suggested previously, ankle sagittal plane motion and peak power generation are generally overestimated using a rigid single-segment model [6]. In our study, the FOOT model overestimated peak power by up to 53% (35% on average, Fig. 5) compared to the MID model. Mid-tarsal joint power is substantial during push-off, and has several likely contributing factors. Actively, the flexor halucis, flexor digitorum, and tibialis posterior on the medial side, and peroneals on the lateral side, act to plantarflex the Forefoot. Yet moment production from these muscles is small [10], and additional contributions likely come from ligamentous restraints and congruency changes in joints of the midfoot. Perhaps more importantly, as the toes extend in terminal stance, the windlass mechanism [11] may increase tension in the plantar fascia resulting in midfoot bone repositioning and plantarflexion. Power absorption at the MP joint with concomitant power generation at the mid-tarsal joint (Fig. 5) suggests energy transfer between the joints.

Sagittal plane motion is likely coupled with coronal and transverse plane motions. Subtalar supination (plantarflexion, inversion, and adduction) changes the orientation of the midfoot

bones, which assists in raising the medial longitudinal arch and plantarflexing the mid-tarsal joint [12]. In our data, we see both ankle and mid-tarsal supination beginning in terminal stance, followed by pronation at both joints when the foot is unloaded in pre-swing (see part I). Substantial ankle eversion power absorption is evident in terminal stance as the medially directed GRF applies a small stress to the lateral ankle tissues. At the mid-tarsal joint, this same effect manifests itself more as abduction power absorption. Non-sagittal plane kinematic and kinetic deviations may be more pronounced in pathological populations.

Several different approaches have been used to measure subarea GRFs, each with its own limitations. Scott and Winter [5] used a miniature force platform, requiring the superposition of many targeted trials to create a full analysis. Giacomozzi and Macellari [13] and MacWilliams et al. [6] combined a pressure mat with a force platform and used a proportionality assumption to estimate subarea forces. While this is a clinically practical approach, there is some concern over the accuracy of the proportionality assumption, particularly for the MP joint [1] and [3]. In the current study, we used targeted walking and two adjacent force platforms to directly measure subarea forces. Previous studies have shown good agreement between targeted and non-targeted GRFs [14] and [15] as well as plantar pressures [16], [17] and [18]. The representative trials were also chosen so as to minimize differences between the targeted virtual ground reaction forces and the ensemble average ground reaction forces from the same subject's non-targeted trials. Analysis of additional kinematic and kinetic variables between targeted and non-targeted walking shows minor differences in specific areas. Overall, the presented ensemble averages appear to be reasonably representative of normal gait.

The split force platform approach of course has its own limitations, particularly if applied to pathological populations. Ground reaction forces were measured under the phalanges collectively, but considered to act entirely on the Hallux segment. Additionally, the joint line in the MP trials ran slightly diagonal to the force platforms, so that the fourth and fifth toes did not always completely cross the platform division. However, the forces on the lesser toes are small in comparison to the force on the Hallux [19] and these limitations should have minimal effects on the results. While targeted walking is an option for some high functioning patients, it is unlikely to be practical for most. Still, several elements of the model can be implemented using a single force platform and incorporated into routine data collection. Accurate ankle joint powers can be calculated throughout the gait cycle using a single segment kinetic model to calculate the joint moment and a Hindfoot kinematic model to calculate angular velocity. Mid-tarsal joint kinetics can also be calculated from a single force platform for the push-off phase of the gait cycle, as the Hindfoot is generally off the ground after terminal stance. While most commercial software is not set up to allow this type of custom analysis, it can be done in some packages using a combination of kinetic and kinematic segments, and low mass dummy segments to control the kinetic chain when needed (e.g. see Fig. 1B). The inclusion of MP joint kinetics and/or mid-tarsal kinetics in early stance may require additional methodology or equipment not currently available [1], [20] and [21]. Additionally, the data and methods presented here can be used to further validate subarea estimation methods such as those mentioned above [6] and [13].

Conclusions

In these companion papers, we have presented and analyzed a simple kinetic multi-segment foot model that is less reliant on assumptions in force measurement and joint motions than those previously presented. While the methodology employed to measure subarea forces is not ideal for pathological gait, some elements of the model can be incorporated into routine analysis. The model and associated normal database may be of benefit in understanding and monitoring pathologies. Specific examples include: insight into the forces causing rocker bottom foot deformity, more accurate determination of muscular contributions to varus hindfoot presentations [22] and tibialis posterior dysfunction [23], and more complete analysis of talipes equinovarus, plantar fasciitis, metatarsus adductus, etc.

Normative gait data presented here shows the importance of the mid-tarsal and MP joints in musculoskeletal models. Clearly, these joints do not function separately, and interactions between the ankle and mid-tarsal joints, and between the mid-tarsal and MP joints should be further studied. In our model, we also did not address force attenuation due to fat pad and soft tissue damping [5], and suggest this be added in future models. The fidelity of musculoskeletal simulations may also be enhanced by more complex measurements of foot and ankle function such as presented here.

References

[1] D.A. Bruening, K.M. Cooney, F.L. Buczek, J.G. Richards. Measured and estimated ground reaction forces for multi-segment foot models. J Biomech, 43 (16) (2010), pp. 3222–3226

[2] F.L. Buczek, M.R. Walker, M.J. Rainbow, K.M. Cooney, J.O. Sanders. Impact of mediolateral segmentation on a multi-segment foot model. Gait Posture, 23 (4) (2006), pp. 519–522

[3] M. Yavuz, G. Botek, B.L. Davis. Plantar shear stress distributions: comparing actual and predicted frictional forces at the foot–ground interface. J Biomech, 40 (13) (2007), pp. 3045–3049

[4] R. Baker, J. Robb. Foot models for clinical gait analysis. Gait Posture, 23 (4) (2006), pp. 399–400

[5] S.H. Scott, D.A. Winter. Biomechanical model of the human foot: kinematics and kinetics during the stance phase of walking. J Biomech, 26 (9) (1993), pp. 1091–1104

[6] B.A. MacWilliams, M. Cowley, D.E. Nicholson. Foot kinematics and kinetics during adolescent gait. Gait Posture, 17 (3) (2003), pp. 214–224

[7] W.T. Dempster. Space requirements of the seated operator. Wright Air Development Center, Wright Patterson Air Force Base (1955)

[8] Hanavan E. A mathematical model for the human body. Wright-Patterson Air Force Base: Technical Report; 1964.

[9] R.P. Wells. The projection of the ground reaction force as a predictor of internal joint moments. Bull Prosthet Res, 10–35 (1981), pp. 15–19

[10] J. Perry. Gait analysis normal and pathological function. SLACK Inc., Thorofare, NJ (1992)

[11] E.A. Fuller. The windlass mechanism of the foot. A mechanical model to explain pathology. J Am Podiatr Med Assoc, 90 (1) (2000), pp. 35–46

[12] H. Elftman. The transverse tarsal joint and its control. Clin Orthop, 16 (1960), pp. 41–46

[13] C. Giacomozzi, V. Macellari. Piezo-dynamometric platform for a more complete analysis of foot-to-floor interaction. IEEE Trans Rehabil Eng, 5 (4) (1997), pp. 322–330

[14] M.D. Grabiner, J.W. Feuerbach, T.M. Lundin, B.L. Davis. Visual guidance to force plates does not influence ground reaction force variability. J Biomech, 28 (9) (1995), pp. 1115–1117

[15] A.E. Patla, C. Robinson, M. Samways, C. Armstrong. Visual control of step length during overground locomotion: task specific modulation of the locomotor synergy. J Exp Psychol Hum Percept Perform, 15 (1989), pp. 603–617

[16] A. Bryant, K. Singer, P. Tinley. Comparison of the reliability of plantar pressure measurements using the two-step and midgait methods of data collection. Foot Ankle Int, 20 (10) (1999), pp. 646–650

[17] T.G. McPoil, M.W. Cornwall, L. Dupuis, M. Cornwell. Variability of plantar pressure data. A comparison of the two-step and midgait methods. J Am Podiatr Med Assoc, 89 (10) (1999), pp. 495–501

[18] B. Meyers-Rice, L. Sugars, T. McPoil, M.W. Cornwall. Comparison of three methods for obtaining plantar pressures in nonpathologic subjects. J Am Podiatr Med Assoc, 84 (10) (1994), pp. 499–504

[19] S.C. Wearing, S.R. Urry, J.E. Smeathers. Ground reaction forces at discrete sites of the foot derived from pressure plate measurements. Foot Ankle Int, 22 (8) (2001), pp. 653–661

[20] B.L. Davis, J.E. Perry, D.C. Neth, K.C. Waters. A device for simultaneous measurement of pressure and shear force distribution on the plantar surface of the foot. J Appl Biomech, 14 (1) (1998), pp. 93–104

[21] J.R. Mackey, B.L. Davis. Simultaneous shear and pressure sensor array for assessing pressure and shear at foot/ground interface. J Biomech, 39 (15) (2006), pp. 2893–2897

[22] M.R. Walker, F.L. Buczek, K.M. Cooney, N.A. Sharkey, J.O. Sanders. Multisegment foot biomechanics in dynamic hindfoot varus
G.F. Harris, P.A. Smith, R.M. Marks (Eds.), Foot and ankle motion analysis – clinical treatment and technology, CRC Press, Taylor and Francis Group, LLC, Boca Raton (2008), pp. 489–508

[23] C. Neville, A. Flemister, J. Tome, J. Houck. Comparison of changes in posterior tibialis muscle length between subjects with posterior tibial tendon dysfunction and healthy controls during walking. J Orthop Sports Phys Ther, 37 (11) (2007), pp. 661–669